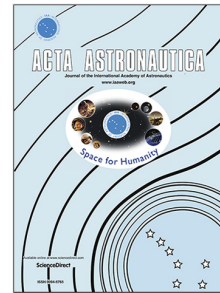# Journal Pre-proof

Spacecraft and optics design considerations for a spaceborne lidar mission with spatially continuous global coverage

Christopher John Lowe, Ciara Norah McGrath, Steven Hancock, Ian Davenport, Stephen Todd, Johannes Hansen, Iain Woodhouse, Callum Norrie, Malcolm Macdonald

Please cite this article as: C.J. Lowe, C.N. McGrath, S. Hancock et al., Spacecraft and optics design considerations for a spaceborne lidar mission with spatially continuous global coverage, *Acta Astronautica* (2023), doi: https://doi.org/10.1016/j.actaastro.2023.10.042.

This is a PDF file of an article that has undergone enhancements after acceptance, such as the addition of a cover page and metadata, and formatting for readability, but it is not yet the definitive version of record. This version will undergo additional copyediting, typesetting and review before it is published in its final form, but we are providing this version to give early visibility of the article. Please note that, during the production process, errors may be discovered which could affect the content, and all legal disclaimers that apply to the journal pertain.

Graphical Abstract

Spacecraft and optics design considerations for a spaceborne lidar mission with spatially continuous global coverage

Christopher John Lowe, Ciara Norah McGrath, Steven Hancock, Ian Davenport, Stephen Todd, Johannes Hansen, Iain Woodhouse, Callum Norrie, Malcolm Macdonald

Highlights

Spacecraft and optics design considerations for a spaceborne lidar mission with spatially continuous global coverage

Christopher John Lowe, Ciara Norah McGrath, Steven Hancock, Ian Davenport, Stephen Todd, Johannes Hansen, Iain Woodhouse, Callum Norrie, Malcolm Macdonald

- Global annual lidar coverage from space is technologically and financially feasible

- Deployable optics significantly increase the value potential of a space lidar mission

- Semiconductor (Diode) lasers are more promising than traditional solid-state lasers

- Fewer, larger platforms generally perform better than many, smaller platforms

- Nano-satellite platforms offer limited value due to their constrained aperture area

Spacecraft and optics design considerations for a spaceborne lidar mission with spatially continuous global coverage

Christopher John Lowe[a], Ciara Norah McGrath[b], Steven Hancock[c], Ian Davenport[c,g], Stephen Todd[d], Johannes Hansen[c,f], Iain Woodhouse[c], Callum Norrie[e], Malcolm Macdonald[a,*]

[a] Applied Space Technology Laboratory (ApSTL), Department of Electronic and Electrical Engineering, University of Strathclyde, 204 George St, Glasgow, G1 1XW, United Kingdom
[b] Space Systems Research Group, School of Engineering, University of Manchester, Oxford Rd, Manchester, M13 9PL, United Kingdom
[c] School of Geosciences, University of Edinburgh, Edinburgh, EH9 3FF, United Kingdom
[d] The UK Astronomy Technology Centre (UKATC), Science and Technology Facilities Council (STFC), Royal Observatory Edinburgh, Blackford Hill, Edinburgh, EH9 3HJ, United Kingdom
[e] Space Flow Ltd, 51/3 Warrender Park Road, Edinburgh, EH9 1EU, United Kingdom
[f] Sylvera Ltd., 20 Chiswell St, London, EC1Y 4TW, United Kingdom
[g] Institute of Science and Environment, The University of Cumbria, The Barn, Rydal Rd, Ambleside LA22 9BB

Abstract

The regular acquisition and delivery of high-resolution, accurate elevation data has historically been provided by airborne lidar (light detection and ranging) solutions, which are costly and highly localised. Providing similar data sets globally has notable scientific and commercial applications, but comes with challenges around scale. In this work, an investigation into such

Corresponding author:
  Email address: malcolm.macdonald.102@strath.ac.uk (Malcolm Macdonald)
  URL: https://www.strath.ac.uk/staff/macdonaldmalcolmdr/ (Malcolm Macdonald)

a service, from low Earth orbit satellites, is presented. The suitability of different space mission architectures is analysed based on platform size and optics mirror design, with the aim of providing true global, high-resolution (5-30m sample resolution) lidar data, annually. The technical challenges, cost implications and feasible solution sets are presented, suggesting that a small number of large platforms offers a cost-effective solution, with the optimal design (of those evaluated) being that of a micro-satellite (~150kg class) constellation with deployed optics capability. Solutions offering relatively low spatial resolution (30m) are lower cost, with the cost rising as a square law with increasing resolution. As platform size continues to decrease, the number of satellites required to maintain global coverage scales exponentially, demanding prohibitively large constellations to ensure global coverage with smaller satellites.

1. Introduction

Lidar (light detection and ranging) is a remote sensing method that uses laser ranging measurements of the Earth to generate precise elevation data. It is a unique remote sensing data source due to its ability to penetrate vegetation cover to provide measurements of bare Earth elevation, and tree canopy height and cover [1, 2]. As a result, lidar data is frequently used in applications such as flood modelling, carbon content mapping, and investi-

gation of archaeological sites [3, 4, 5]. Primarily, lidar surveys are carried out using airborne laser scanning (ALS), however this comes at a relatively high cost per unit ground area, which makes frequent surveying of large areas challenging.

Spaceborne lidar has the potential to enable global mapping at a fraction of the cost of ALS per unit area. However, as an active remote sensing technique, spaceborne lidar must provide its own power for illumination. This requirement results in spaceborne lidars sampling relatively small areas, per unit time, compared to ALS. The Global Ecosystem Dynamics Investigation (GEDI) instrument [2] has the widest swath of any existing spaceborne lidar, but even so, during its four year mission, GEDI's sparse sampling (Figure 1) has resulted in only around 2-4% of the Earth's land surface being directly measured. This results in a standard error of up to 20% per 1 km pixel when estimating above-ground biomass density (AGBD) [2], largely due to the sparse sampling. There is a need for a dataset with lower sampling error and frequent repeats in order to allow precise change detection and to enable applications that require high temporal resolution coverage [6]. These include flood modelling, measuring heterogeneous landscapes such as cities and commercial forests, and precise change detection.

It has been shown that suitable global lidar coverage could be achieved by a constellation of satellites, based on a study of the instrument demands and technology capabilities [7]. It is necessary, therefore, to investigate the technical and financial feasibility of delivering such a service, and understanding the relationship between spacecraft design, lidar coverage and overall cost. This metric of *coverage per unit cost* will be dependent on spacecraft plat-
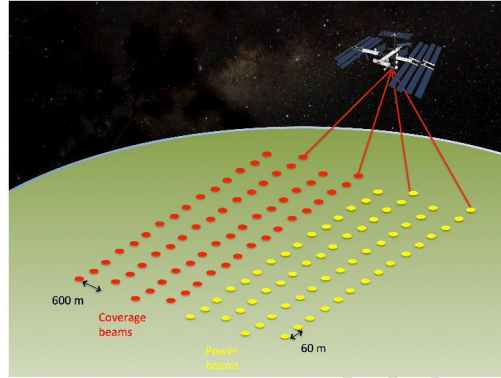
3

Figure 1: Illustration of the sparse sampling technique employed by the GEDI instrument mounted on the International Space Station

form, payload performance, telescope area and mission design. This work presents an investigation into the provision of a global lidar dataset, with the aim of reducing cost while maximising coverage, at different levels of spatial resolution. This is achieved using a combined approach, where spacecraft bus characteristics are obtained through a top-down study of existing platforms, while the required orbital attributes and optics design are met via a bottom-up approach. The results provide insights into the design space, highlighting system- and mission-level trends that can guide future spaceborne lidar development.

Little investigation into mission design for global spaceborne lidar has been done previously. In [8], a tool that can optimize the lidar coverage provided by a satellite constellation to address specific applications was discussed, although the tool has not been made publicly available. Considering

4

the specific application of wind retrieval, [9] considers the potential for a constellation of CubeSat spacecraft equipped with lidar. Their investigation focuses on using three spacecraft to obtain multistatic measurements, rather than considering the possibility of scaling up the constellation to provide global coverage. They also define the spacecraft bus from the outset, and do not investigate the potential of alternative buses.

Previous work by the authors in [7] has derived the equations for calculating the coverage a lidar satellite constellation can achieve for a given set of payload properties against mission requirements. These requirements include payload power, laser efficiency, telescope (primary mirror) area, ground resolution and energy needed for an accurate measurement. Further work in [10] explored different lidar laser sources and modalities, while [11] examines the effect of altitude selection on spaceborne lidar performance, and considers the suitability of very low Earth orbit (VLEO) as an operational regime. In this article, the authors build on results presented in these prior works, by investigating potential solutions that maximise lidar coverage per unit cost, at different levels of resolution performance. Specifically, the primary research question is what platform-optics-constellation design combination offers the most promise of a cost-effective mission to deliver a true global lidar dataset with an annual repeat rate.

2. System Design Assumptions

The requirements for a global-coverage lidar mission selected for this design study are taken from [7]. These are to provide; global land coverage with a temporal resolution (i.e. revisit time) of <1 year; a spatial resolution

5

(i.e. ground sampling distance, GSD) of <30m, and; an 80% confidence of obtaining a cloud-free image over 95% of the land on Earth. The remainder of this article compares the impact of system-level design decisions on the mission architecture in terms of number of spacecraft required and rough order of magnitude (ROM) mission costs. This provides insights into the impact of platform and instrument design choices on the level of global lidar data provision possible.

2.1. Platform Design

To obtain a good understanding of the resources available to a lidar payload (including the optics module), an investigation into available spacecraft platforms has been carried out (29 platforms in total). This information can then be used to inform development of a lidar payload in conjunction with the satellite bus on which it would be hosted. Through this study, the capabilities of busses ranging from nano-satellite (12U CubeSats) to mini-satellite (500kg class) platforms have been analysed. Information has been gathered directly from satellite platform providers, to which "best-fit" relationships are identified for the key performance attributes that impact lidar operation. It should be noted that while every effort has been made to ensure consistency across the data collected, different information formats from the various manufacturers has meant some assumptions were needed. Error margins have been applied in the analysis in an attempt to account for inconsistencies with the data. Furthermore, due to the confidential nature of some of the data obtained from platform providers, the information provided herein is anonymised. Amongst the 29 platforms that have been reviewed, the following data (or a subset of, depending on the platform) was obtained;

6

mass (dry, wet, bus-only and payload-only), volume (total, payload), surface area (each face and available payload aperture area where specified), power (total generated, peak and average available for platform, peak and average available for payload operations), battery capacity, pointing capability (knowledge, pointing accuracy and stability), data storage capacity and download data rate.

The data of most significance for the design and analysis of the lidar payload and optics module in this work are the available volume, mass, aperture surface area and orbit-averaged power for the payload. These are presented in Figures 2 and 3, where each is plotted against overall platform mass. Linear best-fit lines for each dataset provide a guide for the values that could be expected for each payload attribute (mass, volume, aperture surface area and orbit average power). Indeed, outliers in the data do highlight differences between some spacecraft platform designs, however a general trend for each attribute is clear.

Attributes corresponding to a 12U (nano), 150kg-class (micro) and 500kg-class (mini) satellite bus have been extracted from the collected data, for detailed investigation in this work. Metrics for these buses have been identified from a combination of the data in Figures 2 and 3. The bus-specific attributes are summarised in Table 1, which are used for the remaining design and analysis presented in the sections that follow.
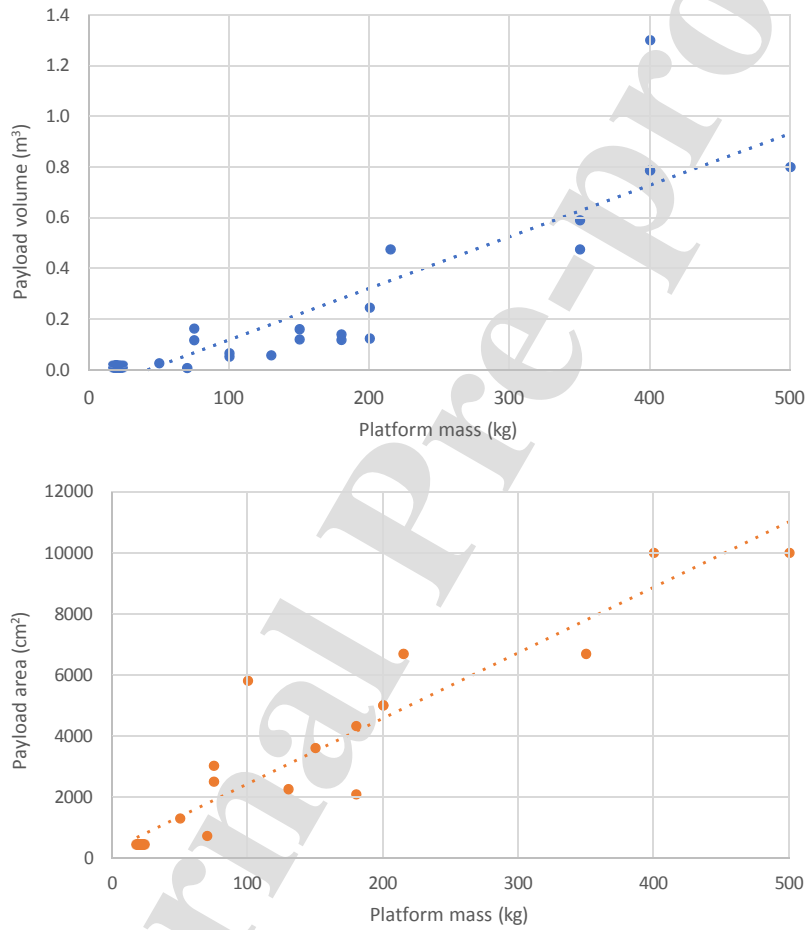
7

Figure 2: Data for off-the-shelf platforms, illustrating the relationship between payload volume (top) and payload area (bottom), against platform mass. Best fit lines provided for clarity.
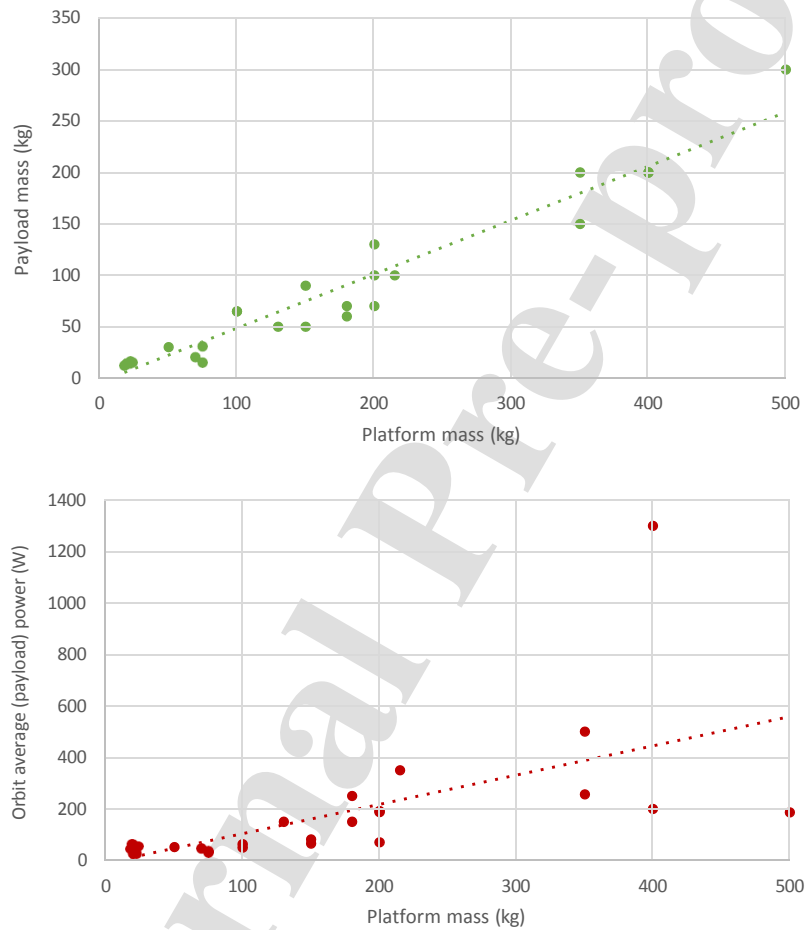
8

Figure 3: Data for off-the-shelf platforms, illustrating the relationship between payload mass (top) and available payload power (bottom right) against platform mass. Best fit lines provided for clarity.

9

Table 1: Platform attributes that have been obtained from the top-down analysis

Attribute	12U	150kg	500kg
Payload volume[1] (m^3)	0.008 (8U)	0.2	0.8
Payload area[2] (m^2)	0.031	0.28	0.64
Payload mass (kg)	14	75	250
Peak power[3] (W)	115	250	500
Average power[4] (W)	40	160	300
Downlink rate (Mbps)	100	250	400

[1] *"Payload volume" is assumed to be cube-like, although different options exist on specific platforms for alternative payload geometries.*

[2] *"Payload area" is considered to be the maximum size of circular optical aperture that could be accommodated on the surface expected to be Earth-facing.*

[3] *"Peak power" is assumed to be the maximum available power for use by the payload for a short duration.*

[4] *"Orbit average power" is the long-term average power available to the payload*

2.2. Lidar payload

For this study, two different types of lidar instrument were considered. Existing spaceborne lidars use solid-state lasers which have a long space heritage and are traditionally capable of 5-8% efficiency and more recently shown to reach up to 11%, in [12]. Recent work suggests that semiconductor lasers, with potential efficiencies of up to 25% but lower peak powers than solid-state lasers, could be used in satellite lidar in a pulse-train mode [10]. Semiconductor lasers are also known as laser diodes and differ from solid-state lasers. In solid-state lasers, such as Nd:YaG, light energy (often itself from a diode) is used as the pump source for a lasing medium whereas, in semiconductor (diode) lasers, electrical energy is used as the pump source. The relevant parameters of these laser options are given in Table 2 and defined in full in [10], which are used as part of the trade-study presented in section 3.

Table 2: Laser parameters. All values taken from [10]

Attribute	Solid-state	Diode
Wavelength.	1064 nm	850 nm
Surface reflectance (ρ)	0.42	0.32
Atmospheric transmittance (τ)	85 %	80 %
Energy detected at receiver (E_{det})	0.014 fJ	0.027 fJ
Detector quantum efficiency (Q)	31 %	58 %
Laser Power conversion efficiency (L_E)	11 %	25 %

11

2.3. Optics

The telescope area controls how much light is collected by the satellite and so is directly proportional to the swath width achievable by a lidar satellite [7]. Fixed and deployable optics were considered and conceptual optical designs were developed for each of the three satellite platform classes described above. In each case the aim is to maximise the collecting area of the telescope. Within this study, we consider only a simple volume for each platform class – more detailed space envelopes will depend on the complete system design (spacecraft and payload).

Given the peak instantaneous and average power limits of diode lasers [10], it is assumed that each laser will illuminate a single footprint and be imaged by a single detector; as such, a scanning or beam-splitting system is not considered suitable for diode lasers. It can be used with solid-state lasers. The laser spots can be staggered along the direction of travel to increase the separation on the ground, but the collecting optics must still operate as a low resolution imaging system, with sufficient optical quality to minimise cross-talk between spots (figure 4, right hand image).

The use of deployable optics may allow a substantial increase in collecting area and hence system efficiency for a given satellite platform size [13, 14]. In this case the goal is to collect as much return energy as possible, rather than the more usual aim to increase the diffraction limited resolution. For a deployed system, a number of mirror segments would be folded into a stowed position within the platform volume for launch and then deployed in orbit to form a total collecting area larger than the available platform cross-section (Figure 5).
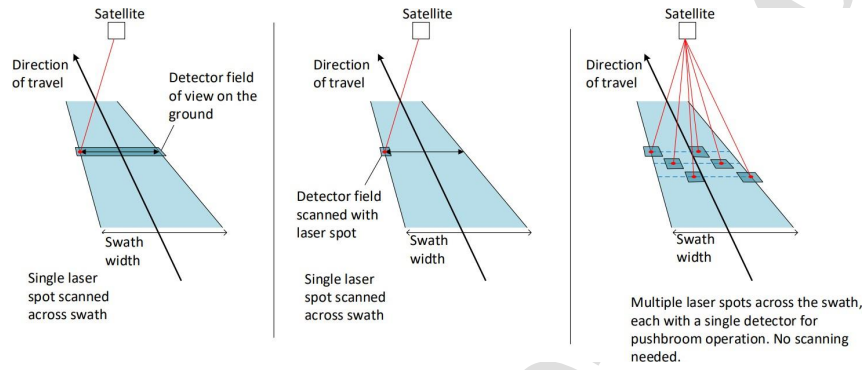
12

Figure 4: A schematic view of three operating modes suitable for spaceborne lidar. Note than only the method on the right is considered for diodes lasers in this study.

The deployable optics designs considered in this study, are such as that illustrated in 5. Both "2-segment" and "4-segment" configurations are evaluated, each resulting in an increase in telescope collection area proportional to the increase in area from which the reflected signal is acquired. This additional area is realised through the use of either two, or four sides of the platform opening up to act as reflective surfaces, respectively. The effective aperture area results of this design exercise are shown in Table 3. Note that while the authors' knowledge of deployed optics for nano- and micro-satellites is sufficient to estimate rough order magnitude (ROM) cost of development, it was decided to omit this option for 500 kg mini-satellites, to minimise risk of presenting inaccurate information.
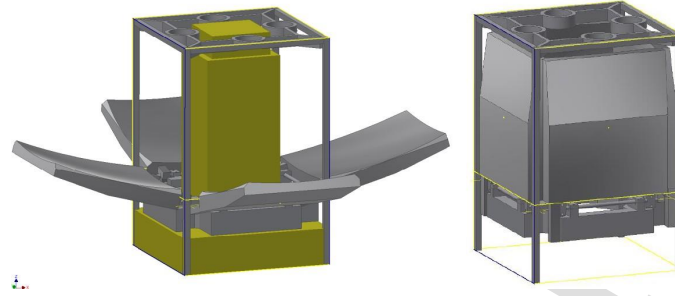
13

Figure 5: Example of deployed optic configuration, showing the 4-deployed Cassegrain option for a 12U nano-satellite bus

Table 3: Maximum calculated payload aperture area for each platform class and deployed optics configuration

	Aperture area (m^2)		
Optics type	12U (nano)	150kg (micro)	500kg (mini)
Body-mounted	0.03	0.25	0.6
2-segment	0.058	0.5	-
4-segment	0.115	1.0	-

3. Methodology

This section outlines the methodology to calculate the number of spacecraft required to meet specific levels of performance (spatial and temporal resolution) for varying platform, laser and optics combinations. The cost modelling approach is also outlined, offering the necessary inputs for comparing designs from an overall mission value perspective. Outputs from the performance and cost models are used to identify optimal mission configura-

14

tions from the discrete set of combinations considered and provide insights into the design space for a spaceborne lidar system providing global coverage.

3.1. Constellation Sizing

The constellation sizing method used builds on the approach introduced by the authors in [7], which takes into consideration the coverage provided by individual platforms based on their hosted payload attributes, and historical cloud cover information across a discrete, globally distributed set of land-based locations.

Following the method in [7], the number of spacecraft (N_p) required to provide coverage (i.e. cloud-free data acquisition) at a specific latitude (δ) and longitude (λ), in a given time (t) and with a desired level of observation confidence (p_{obs}), can be found using equation (1). The equation can be evaluated for a number of discrete latitude and longitude points of interest, generating an understanding of how constellation sizing differs in different global regions. For this work, only latitude/longitude points corresponding to land are considered.

$$N_p\left(\delta, \lambda\right) = \frac{1}{W\left(\delta\right) - 2h\psi} \frac{c\left(\delta\right)\pi\sqrt{\left(R + h\right)^3}}{t\sqrt{\mu}} \frac{\ln\left(1 - p_{obs}\right)}{\ln\left(c_{frac}\left(\delta, \lambda\right)\right)} \tag{1}$$

In equation (1), R is the radius of the Earth, t is the time to achieve global coverage in seconds, h is the platform altitude, $c_{frac}(\delta, \lambda)$ is the mean probability of cloud cover for a given point of the Earth[1], $c(\delta)$ is the circumference

---

[1]Cloud cover data was obtained from the 2007 data from Cloud-Aerosol Lidar and Infrared Pathfinder Satellite Observation (CALIPSO) Cloud-Aerosol LIdar with Orthogonal Polarization (CALIOP) instrument [15]

15

of the latitude band for the point being considered and $W(\delta)$ is the projected width of the spacecraft swath along a latitude band δ. This width is calculated as $W = \frac{s}{\sin\beta}$ where s is the swath width of the lidar as calculated using equation 2.5 in [7], and $\beta = \tan^{-1}\left(\frac{\sqrt{\sin^2 i - \sin^2 \delta}}{\cos i - \omega \cos^2 \delta}\right)$, where i is the orbit inclination and ω is the rotation rate of Earth. An addition to equation (1) from the method presented in [7] is the inclusion of the platform pointing accuracy (ψ), which defines the required overlap between adjacent passes to compensate for pointing inaccuracies.

To calculate the number of satellites required to provide 80% confidence in coverage over 95% of land globally, equation (1) is executed for a large number of (evenly distributed) points on the Earth (land only). From this set of results, the most demanding 5% (i.e. the set of results with largest constellation size requirements) are ignored and the worst-case result (highest number of satellites) is selected from the data that remains. This number of satellites is thus what is necessary to ensure coverage is achieved at the defined level of confidence. Note that evenly distributed ground locations have been used, to maintain consistency with the area represented by each point.

There is a chance, particularly for smaller platforms with less payload power and telescope aperture, for the swath width of the image (W) to be less than the required overlap ($2h\psi$). This would result in a negative number of satellites being outputted from equation (1). These options are ignored, since they do not offer a feasible solution to lidar data acquisition given the properties used in this work.

16

3.2. Cost Modelling

To understand true mission value, and thus compare platforms and constellations of different configurations, it is important to consider cost, as well as performance. Often, cost is not only financial, and could include developmental, technical, business and political considerations. However, for the purposes of this study, a rough order of magnitude (ROM) financial cost of building, launching and operating each mission architecture is used. This is considered a reasonable first step towards understanding general trends across design architectures. The aim here is to understand general trends related to lidar coverage and cost, amongst different platform and constellation configurations, which can be used to inform lower-level research going forward.

Overall mission cost for each design configuration is approximated as the sum of the costs associated with the satellite optics (Section 3.2.1), platform (Section 3.2.2), launch (Section 3.2.3) and operation (Section 3.2.4) (i.e. data download). The authors acknowledge that there are numerous elements not considered here, which could have significant impact on the overall cost values.

3.2.1. Optics Cost

Cost estimates for the optics are presented in Table 4, for each satellite class, broken down into fixed, two-segment and four-segment deployed designs. While the values presented here are early phase estimates, based on a combination of both parametric and bottom-up cost analyses from years of space optics design and development experience (at the UK Astronomy Technology Centre), they serve as a useful input to the overall mission cost.

17

These costs are recurring, such that they are considered on a per-platform basis in the analysis that follows.

Table 4: Optics cost for different platform types and optics designs

Platform	Cost (k$, US)		
	Fixed	2-segment	4-segment
12U	481	624	806
150kg	844	1,064	1,897
500kg	1,340	-	-

3.2.2. Platform Cost

In order to estimate the unit cost of each spacecraft platform in the constellation (not including the payload or optics module), a bulk order discounted cost model is proposed. This approach accounts for a reasonable level of cost reduction with the purchase of multiple units, and is based on discussions with platform providers. The cost of each bus is therefore a function of the total number of spacecraft manufactured N, with a baseline cost c_b of \$1M for a 12U platform, \$10M for 150kg class and \$25M for 500kg class (all costs in US dollars). This relationship is defined as

$$c_{bus} = \max\left(c_b\left(1 - \frac{N-1}{2n_{50\%}}\right), \frac{c_b}{2}\right) \tag{2}$$

where $n_{50\%}$ is the number of additional platforms at which a 50% discount is reached. For the purposes of this work, $n_{50\%} = 99$, such that 100 platforms would result in a 50% discount per platform, and it is assumed that a 50% discount on the baseline cost is the minimum unit cost achievable. This

18

effectively results in a linear decrease in cost per platform, with increasing platform numbers, to a minimum of half that of the nominal platform cost.

3.2.3. Launch Cost

Launch costs are estimated for each platform class based on costs published by a rideshare launch provider [16], and extrapolated where necessary to provide an estimate. Figure 6 illustrates indicative pricing as of the time of writing. Based on this information, launch of a single spacecraft (on a ride-share opportunity) would cost \$595kUS, \$1,350kUS and \$2,200kUS for a 12U (~20kg), 150kg and 500kg spacecraft, respectively.
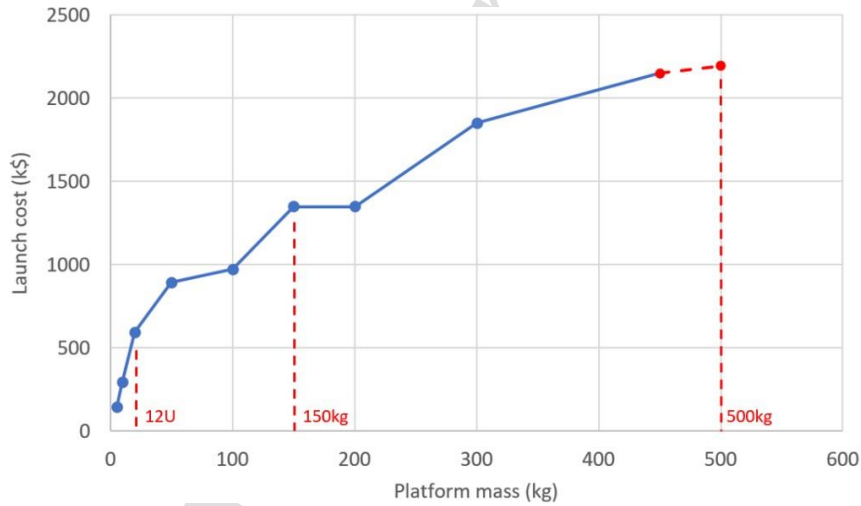

Figure 6: Estimated rideshare launch cost for different spacecraft masses (data provided up to 450kg spacecraft, so extrapolation up to 500kg shown in red-dash)

If launching a constellation of satellites, it is anticipated that some saving would be possible if using a large proportion of the launch vehicle, however

19

there may also be some additional cost associated with reaching a specific orbit that suits the needs of a global lidar mission. As such, it is proposed that the above figures provide a good ROM launch cost, without discounts applied.

3.2.4. Operations Cost

Operations cost (C_{ops}) is defined here as the annual cost incurred to retrieve data acquired during operations. In this study, this is calculated as

$$C_{ops} = \frac{V_L C_{GS}}{L R_{dl}}, \tag{3}$$

where V_L is the volume of data acquired over the repeat period (L, in seconds), C_{GS} is the cost of Ground Station access per second, which could be a function of the download data rate depending on provider and R_{dl} is the rate of data download. For ground station services such as those provided by Amazon Web Services (AWS), where contact time can be reserved in advance at a fixed rate, the upfront cost of building ground segment infrastructure can be avoided, with a trade-off of higher recurring costs. AWS offers a reserved slot download service at a cost (C_{GS}) of \$10US per minute (at the time of writing), which shall used in this study. Other providers, e.g. Leaf Space and Microsoft Azure, also offer *Ground Station as a Service* (GSaaS) products, such that discounted rates for large data volumes are considered likely, but not explored here.

The download data rate (R_{dl}) will vary depending on the platform size, where rates of 100Mbps, 250Mbps and 400Mbps are assumed as baselines for 12U, 150kg and 500kg platform classes, respectively (based on information from the platforms evaluated).

20

The volume of data acquired over the course of a mission repeat cycle (1 year, in the case of this investigation) is dependent on the resolution of the instrument. To minimise the volume of data being downloaded and therefore the operations cost, data associated with a specific ground location is considered to be downloaded only once. This would require on-board autonomous data processing in order to identify cloud-free pixels, which is a reasonable assumption for a future mission as such technologies are being developed [17]. An approximation of the total data volume (V_L) generated during a repeat cycle can be defined as

$$V_L = \frac{1.2 A_E V_{pix}}{r_{gsd}^2},$$

(4)

where V_{pix} is the data volume of a single pixel (16kb in this work), A_{Earth} is the total surface area of the Earth covered by land ($\sim$150Mkm^2) and r_{gsd} is the resolution of a single pixel. It should be noted that this is a simplified model whereby each pixel is assumed to represent a square area on the ground of side length equal to the resolution value, e.g. 10m resolution (ground sample distance, GSD) would represent pixels of 10m x 10m in area. A factor of 1.2 is applied to capture image overlap and data overhead.

The annual cost of operations for a 1-year global revisit period are shown in Figure 7 as a function of download data rate, assuming use of the AWS ground station services. As defined in Equation (4), the volume of data, and therefore the cost to download, increases with the inverse of the square of GSD, which is reflected in the significant increase as GSD decreases from 30m to 5m. A shorter revisit period would simply result in a linear respective growth in operations cost. For example 1 year to global coverage would be 5 times the cost, per year, of a mission providing 5-years to global coverage.

21

Also clear is the trend of cost reduction for larger platforms, due to their higher rate of data download and, subsequently, lower demand on ground station utilisation.
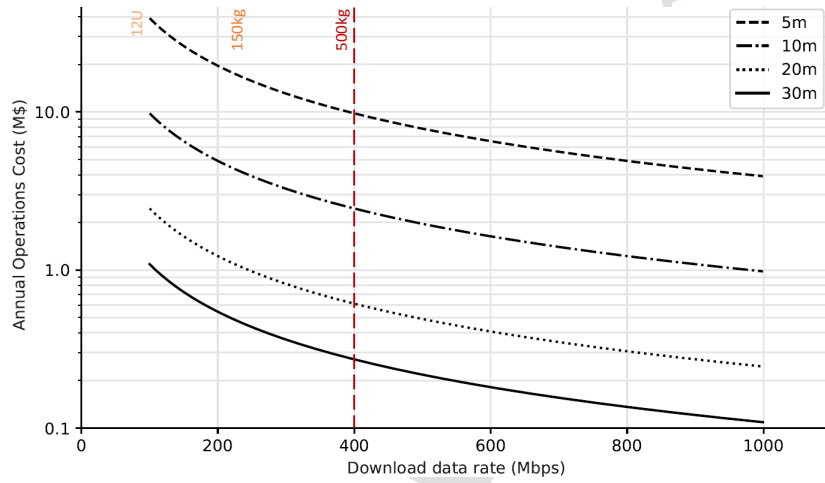

Figure 7: Annual operations cost for different spatial resolutions as a function of download data rate with a global revisit period of 5 years (note log scale on y-axis)

4. Results

The results of the analysis defined in the previous sections is shown below, giving insights into the general trends and relative value for the provision of global lidar data across a range of resolutions from a range of space mission configurations. Value, in this context, is considered the level of performance (spatial resolution) per unit cost, calculated for a 5-year total mission duration, such that coverage is guaranteed over 95% of land, with an 80% probability of delivering a cloud-free image. In the following sub-sections,

22

constellation size shall be established (Section 4.1), representing the number of satellite platforms required to provide lidar data at a temporal resolution (repeat period) of 1-year. Consideration of build, launch and operations cost provide input to the analysis.

4.1. Constellation Size

Analysis has been carried out to identify the number of spacecraft required to obtain global coverage at the level of service defined in the previous section. These results are provided in Table 5, for each combination of platform class (12U, 150kg and 500kg), optics design (fixed, 2-segment and 4-segment), spatial resolution (5m, 10m, 20m and 30m), and laser type (Solid-state and Diode), all at an orbit altitude of 400km. Note, the 500kg platform is considered with only fixed optics, due to the ample laser collecting area available on this platform. The altitude of 400km has been selected as a baseline for comparison as it offers good resolution and coverage performance, without the demanding orbit maintenance of lower altitude orbits, which would require propulsion systems that would significantly impact the platform design [11]. Dashed cells indicate infeasible solutions due to the theoretical swath width being less than the required resolution [7].

It is clear that the nano-satellite (12U) platform lacks the collection area to achieve a swath width narrow enough to achieve 5m resolution, regardless of optics configuration. Acquisition at 10m resolution is feasible for some configurations, with the Diode laser setup providing a solution from a 2-segment deployed arrangement. Generally speaking, platforms with the Diode laser payload have a wider swath, resulting in fewer platforms required to meet specific resolutions. This is due to the increased detector quantum efficiency

23

and laser power conversion efficiency being sufficiently higher in the Diode payload, to offset the requirement for higher energy to be detected at the receiver [7].

Table 5: Number of spacecraft required for 95% global land cover with 80% confidence in 1 year. Cells containing "–" indicate infeasible solutions due to minimum swath width limitations

	Number of platforms required							
	Solid-state				Diode			
Resolution (m)	5	10	20	30	5	10	20	30
12U Cubesat	–	–	555	143	–	–	261	87
12U Cubesat 2-segment	–	–	176	64	–	1574	104	41
12U Cubesat 4-segment	–	614	74	30	–	280	47	20
150 kg platform	159	31	8	4	95	21	5	3
150 kg 2-segment	67	15	4	2	43	10	3	2
150 kg 4-segment	31	8	2	1	21	5	2	1
500 kg platform	28	7	2	1	18	5	2	1

4.2. Mission Cost

Using the platform counts from Table 5 and the costing relationships outlined in Section 3.2, the total cost (including launch and operations costs) for each feasible mission configuration is calculated and presented in Table 6. Costs for configurations that were infeasible due to swath width limitations (i.e. the dashed cells in Table 5) are omitted for clarity and dashed in the table.

24

As expected, the missions with greater number of platforms required to provide complete coverage annually at smaller bus size, have the greatest overall cost, with nano-satellites meeting mission requirements at the highest cost. Generally speaking, the reduction in platform count more than offsets the increased platform cost as bus size increases, with deployed optics offering a cost-effective way to increase performance without significant additional cost. The additional risk and complexity of including deployed optics must be considered in future work, however this initial study suggests there is merit in this technology for this application.

Table 6: Mission cost for 95% global land cover with 80% confidence in one year. Cells containing "–" indicate infeasible solutions due to minimum swath width limitations

	Mission cost (M\$, US)							
	Solid-state				Diode			
Resolution (m)	5	10	20	30	5	10	20	30
12U Cubesat	–	–	753	196	–	–	361	130
12U Cubesat 2-segment	–	–	260	114	–	2264	159	83
12U Cubesat 4-segment	–	969	141	70	–	468	105	50
150 kg platform	1155	347	99	50	748	253	65	38
150 kg 2-segment	663	194	54	27	511	139	42	27
150 kg 4-segment	433	122	31	15	331	85	31	15
500 kg platform	748	206	60	30	522	152	60	30

To illustrate the general trends, mission cost values are plotted against spatial resolution for each platform type (represented by different color families) for the Diode laser payload, with bubble size representing launch mass

25

to orbit (value scales according to bubble area) and the bubble centers representing the value relative to the x-y axes (Figure 8). It is clear that the micro (150kg) class platform with a 4-deployed optics configuration offers the lowest mission cost at all resolution levels (dark-blue bubbles).
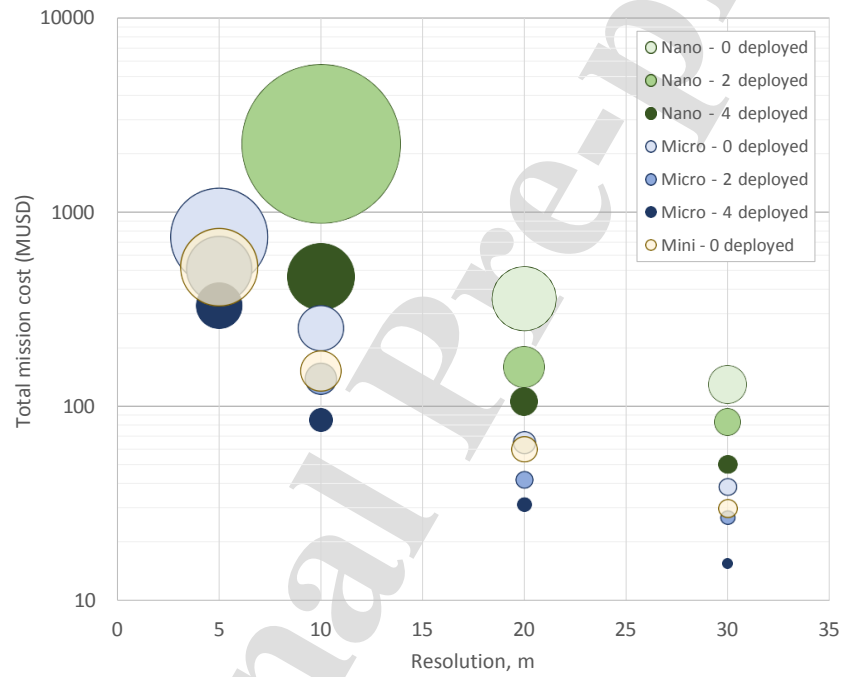

Figure 8: Mission cost vs. spatial resolution, for each platform configuration (log scale on y-axis), with Diode laser payload. Bubble size illustrates relative total mass of the constellation. Note: results for "Mini - 0 deployed" data is transparent to show the hidden results behind it.

5. Conclusions

From the analysis presented here, it is evident that at very small platform scales (12U, nano-satellite), challenges exist on the provision of global lidar data coverage at a competitive cost. For very high spatial resolution imagery (5m), nano-satellites do not exhibit feasible swath widths (i.e. swath narrower than the target resolution), however data at 10m - 30m resolution is possible. The number of platforms required, and thus the overall mission costs, decreases exponentially with increasing ground sampling distance, due to the squared relationship between the swath width and sampling distance, resulting in larger satellites offering greater mission value, despite their higher unit cost. This result is supported by the decrease in operations cost for larger platform constellations, as both the number of satellites demanding ground resources decreases and rate of data download increases. Additionally, as platform size increases, a greater payload aperture area affords the collection of more signal and therefore enables coverage with decreasing numbers of platforms. Deployed optics further increase mission value, by offering a cost-effective way to increase collection area and, therefore, ground coverage. Micro-satellites, with mass on the order of 150kg are seen to benefit significantly from deployed optics technology, and combined with relatively low operations cost, may present the most attractive performance to cost ratio. Development in small-satellites, optics technology and photonics, make a satellite lidar system with spatially continuous global repeat coverage possible.

6. Acknowledgments

References

[1] G. Sun, K. Ranson, D. Kimes, J. Blair, K. Kovacs, Forest vertical structure from glas: An evaluation using lvis and srtm data, Remote Sensing of Environment 112 (1) (2008) 107–117. doi:10.1016/j.rse.2006.09.036.

[2] R. Dubayah, J. B. Blair, S. Goetz, L. Fatoyinbo, M. Hansen, S. Healey, M. Hofton, G. Hurtt, J. Kellner, S. Luthcke, et al., The global ecosystem dynamics investigation: High-resolution laser ranging of the earth's forests and topography, Science of Remote Sensing 1 (2020) 100002. doi:10.1016/j.srs.2020.100002.

[3] D. Coles, D. Yu, R. L. Wilby, D. Green, Z. Herring, Beyond 'flood hotspots': modelling emergency service accessibility during flooding in york, uk, Journal of hydrology 546 (2017) 419–436. doi:10.1016/j.jhydrol.2016.12.013.

[4] A. T. Hudak, E. K. Strand, L. A. Vierling, J. C. Byrne, J. U. Eitel, S. Martinuzzi, M. J. Falkowski, Quantifying aboveground forest carbon pools and fluxes from repeat lidar surveys, Remote Sensing of Environment 123 (2012) 25–40. doi:10.1016/j.rse.2012.02.023.

[5] Ł. Banaszek, D. C. Cowley, M. Middleton, Towards national archaeolog-

28

ical mapping. assessing source data and methodology—a case study from scotland, Geosciences 8 (8) (2018) 272. doi:10.3390/geosciences8080272.

[6] T. C. Hill, M. Williams, A. A. Bloom, E. T. Mitchard, C. M. Ryan, Are inventory based and remotely sensed above-ground biomass estimates consistent?, PLoS One 8 (9) (2013) e74170. doi:10.1371/journal.pone.0074170.

[7] S. Hancock, C. McGrath, C. Lowe, I. Davenport, I. Woodhouse, Requirements for a global lidar system: spaceborne lidar with wall-to-wall coverage, Royal Society open science 8 (12) (2021) 211166. doi:10.1098/rsos.211166.

[8] D. A. Paige, Small satellite constellations for lidar monitoring forest ecosystems, ice, and global change, in: AGU Fall Meeting Abstracts, Vol. 2016, 2016, pp. B54B–06.

[9] D. Josset, Y. Hu, F. Hovis, C. Weimer, W. Hou, J. Pelon, N. Pascal, C. Michael, Measurement of wave slope asymmetry from a multistatic space lidar constellation: Theory and preliminary analysis of wind direction retrievals, in: 2019 IEEE/OES Twelfth Current, Waves and Turbulence Measurement (CWTM), IEEE, 2019, pp. 1–9. doi:10.1109/CWTM43797.2019.8955257.

[10] J. Hansen, S. Hancock, L. Prade, G. Bonner, H. Chen, I. Davenport, B. Jones, M. Purslow, Assessing novel lidar modalities for maximizing coverage of a spaceborne system through the use of diode lasers, Remote Sens. 14 (2022) 2426. doi:10.3390/rs14102426.

[11] C. McGrath, C. Lowe, M. Macdonald, S. Hancock, Investigation of very low earth orbits (vleos) for global spaceborne lidar, CEAS Space Journal (2022). doi:10.1007/s12567-022-00427-2.

[12] J. B. Abshire, X. Sun, E. M. Mazarico, J. W. Head, A. W. Yu, J. D. Beck, A 3-d surface imaging lidar for mapping mars and other bodies from orbit, 2020.

[13] N. Schwartz, W. Brzozowski, M. Milanova, K. Morris, S. Todd, Z. Ali, J.-F. Sauvage, A. Ward, D. Lunney, D. MacLeod, High-resolution deployable CubeSat prototype, in: Space Telescopes and Instrumentation 2020: Optical, Infrared, and Millimeter Wave, Vol. 11443, SPIE, 2020. doi:10.1117/12.2562255.

[14] D. Dolkens, J. M. Kuiper, A deployable telescope for sub-meter resolutions from microsatellite platforms, in: International Conference on Space Optics — ICSO 2014, Vol. 10563, SPIE, 2017. doi:10.1117/12.2304245.

[15] D. M. Winker, M. A. Vaughan, A. Omar, Y. Hu, K. A. Powell, Z. Liu, W. H. Hunt, S. A. Young, Overview of the calipso mission and caliop data processing algorithms, Journal of Atmospheric and Oceanic Technology 26 (11) (2009) 2310–2323. doi:10.1175/2009JTECHA1281.1.

[16] Spaceflight, Pricing information, Accessed on: 14/06/2021, available: https://spaceflight.com/pricing/ (2021).

[17] G. Giuffrida, L. Diana, F. de Gioia, G. Benelli, G. Meoni, M. Donati, L. Fanucci, Cloudscout: A deep neural network for on-board

cloud detection on hyperspectral images, Remote Sensing 12 (14) (2020). doi:10.3390/rs12142205.

UniversityofStrathclyde,UK

Applied Space Technology Laboratory (ApSTL),
DepartmentofElectronicandElectricalEngineering
UniversityofStrathclyde,204GeorgeSt,Glasgow,G11XW,UnitedKingdomchristopher.lowe@strath.ac.uk/malcolm.macdonald.102@strath.ac.uk(corresponding author)
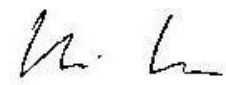
6thAug2023

DearProfessorRockJeng-ShingChern,

Pleasefindbelow,highlightsforthepaper"Spacecraftandopticsdesignconsiderationsforaspacebornelidarmissionwithspatiallycontinuousglobalcoverage".

1. Globalannuallidarcoveragefromspaceistechnologicallyandfinanciallyfeasible
2. Deployableopticssignificantlyincreasethevaluepotentialofaspacelidarmission
3. Semiconductor(Diode)lasersaremorepromisingthantraditionalsolid-statelasers
4. Fewer,largerplatformsgenerallyperformbetterthanmany,smallerplatforms
5. Nano-satelliteplatformsofferlimitedvaluedue totheirconstrainedaperturearea

Sincerely,

ChristopherLowe,PhD

Declaration of interests

☒ The authors declare that they have no known competing financial interests or personal relationships that could have appeared to influence the work reported in this paper.

☐ The authors declare the following financial interests/personal relationships which may be considered as potential competing interests: